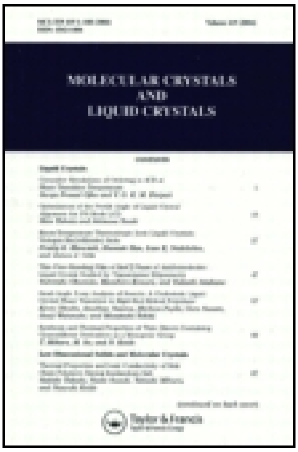

Molecular Crystals and Liquid Crystals Science and Technology. Section A. Molecular Crystals and Liquid Crystals

Publication details, including instructions for authors and subscription information:
http://www.tandfonline.com/loi/gmcl19

# Dielectric Relaxations of a Side Chain Liquid Crystal Homopolymer and Copolymer

R. B. Akins [a] [b] , Z. Z. Zhong [a] , W. L. Gordon [a] & D. E. Schuele [a]

[a] Department of Physics, Case Western Reserve University, Cleveland, Ohio, 44106-7079, U.S.A.

[b] Current address: Motorola Inc., 8000 W. Sunrise Boulevard, Fort Lauderdale, Florida, 33322

Version of record first published: 23 Sep 2006.

To cite this article: R. B. Akins , Z. Z. Zhong , W. L. Gordon & D. E. Schuele (1995): Dielectric Relaxations of a Side Chain Liquid Crystal Homopolymer and Copolymer, Molecular Crystals and Liquid Crystals Science and Technology. Section A. Molecular Crystals and Liquid Crystals, 258:1, 15-26

To link to this article: http://dx.doi.org/10.1080/10587259508034544

*Mol. Cryst. Liq. Cryst.*, 1995, Vol. 258, pp. 15–26
Reprints available directly from the publisher
Photocopying permitted by license only

# Dielectric Relaxations of a Side Chain Liquid Crystal Homopolymer and Copolymer

R. B. AKINS,† Z. Z. ZHONG, W. L. GORDON and D. E. SCHUELE

*Department of Physics, Case Western Reserve University, Cleveland, Ohio 44106-7079, U.S.A.*

*(Received October 1, 1993; in final form April 6, 1994)*

The dielectric loss spectrum of a side chain liquid crystal polymer (SCLCP) has been measured from 10 Hz to 100 kHz in the smectic phase. Three liquid crystalline siloxane polymers are examined, a homopolymer and two random copolymers, all of which contain a chiral smectic mesogen and an eleven-methylene spacer in the side chain. Two dielectric relaxations have been observed, the high-frequency $\alpha$ and low-frequency $\delta$ processes. The effect of the copolymer morphology in these SCLCPs is to increase the dielectric relaxation strength of the $\delta$ process relative to the $\alpha$ process and to cause increased overlap between the two peaks. These two observations suggest that the copolymer structure aids large scale reorientations in the $\delta$ process because of increased cooperativity with the backbone.

*Keywords: Liquid crystal polymer, dielectric relaxation, glass transition, polymer backbone, Fuoss–Kirkwood function.*

## INTRODUCTION

Side chain liquid crystal polymers (SCLCPs) have received a great deal of attraction in recent years both as novel materials and as potential applications for information storage.[1–4] SCLCPs combine the desirable mechanical properties of polymers with the electro-optic properties of low-molar-mass liquid crystals. In the SCLCP geometry liquid crystal mesogens are attached to a polymer backbone via flexible spacers, usually alkyl chains. The mesogens and spacers form pendant side groups off the polymer backbone, giving the molecule a *comb*-shaped structure. The flexible spacers serve to mechanically decouple the mesogens from the backbone so that the mesogens can reorient with minimal re-ordering of the polymer backbone. At low temperatures SCLCPs are either semi-crystalline or glassy. Above a certain temperature, usually the glass transition temperature, they exhibit liquid crystalline mesophases, i.e., nematic, smectic, cholesteric, etc.[5,6]

To enhance the decoupling of the backbone and mesogenic units in such a side-chain system, Percec and co-workers have synthesized a series of poly(methylsiloxane) based SCLCPs containing heterocycloalkanediyl mesogens as both a homopolymer and several random copolymers with poly(di-methylsiloxane).[4,7–10] In the copolymers a spacer and mesogen is attached to only a certain percentage of the backbone units. In the *comb* analogy the copolymer appears as a comb with random teeth missing. They have suggested that the two changes in heat capacity in the copolymers are most

---

† Current address: Motorola Inc., 8000 W. Sunrise Boulevard, Fort Lauderdale, Florida 33322.

probably associated with two glass transition temperatures. One glass transition temperature is assigned to the independent motion of the polymer backbone and the other to the cooperative (but independent from the polymer backbone) motion of the side groups. Therefore, these copolymers should exhibit an intramolecular microphase-separated morphology.[11] Extrapolation of these two glass transition temperatures suggest that the poly(methylsiloxane) containing mesogenic side groups may also exhibit two glass transition temperatures.[10]

There has been a great deal of interest in dielectric studies for SCLCPs.[12–14] Most SCLCPs show two dielectric relaxations in mesophases right above the glass transition temperatures. In all recent studies based on rotation dynamic theory,[15–18] these two relaxations are referred to as $\delta$ and $\alpha$ processes in decreasing temperature. At a given temperature the $\alpha$ process occurs at higher frequency than the $\delta$ process. The $\delta$ process is essentially associated with the rotation of the longitudinal dipole moment in the mesogen about the short axis of the uniaxial mesogen. In smectic phases, this implies that the mesogen may possibly rotate about the polymer backbone, hopping from one smectic layer to another. The $\alpha$ process is thought to be a combination of a few rotational reorientation modes, dominated by the rotation of the transverse dipole moment about its long axis. Some portions of polymer backbone may also contribute to the $\alpha$ process, however debate remains on this point.[19–21] Other than the nature of the glass transition of the backbone, these assignments have been largely confirmed in the past several years by studies on homeotropic and planar aligned samples.[20,21]

Haws *et al.* have made dielectric studies on a series of copolymers having mesogenic side groups on the average attached to 21/40 methylsiloxane backbone units with various spacer lengths and mesogens.[22] Two equivalent homopolymers were also studied. In their study one homopolymer/copolymer pair is designated GN3/17 and Gn3/18, the other pair is designated "A" and GN3/16.[23] The work was done on unaligned samples and the dielectric data was fitted to Fuoss–Kirkwood functions.[24] For the pair GN3/17 and GN3/18 at $T = 0.95\,T_c$, where $T_c$ is the clearing temperature, both $\alpha$ and $\delta$ relaxations appeared at lower frequencies for the copolymer than for the homopolymer. The authors attributed this to a relatively high microviscosity in copolymer GN3/18. The decrease in relaxation frequency was greater for the $\alpha$ peak, resulting in the two peaks becoming more overlapped in the copolymer. In the pair "A" and GN3/16 at $T = 0.92\,T_c$, the narrow $\delta$ process was also at a lower frequency. However the $\alpha$ process appeared at a higher frequency in the copolymer, resulting in the peaks becoming less overlapped. In this case the copolymer structure presented less hindrance to the motion of mesogenic dipole components.

In this article, we will examine one poly(methylsiloxane) based homopolymer containing a chiral smectic mesogen and two corresponding copolymers, consisting of 35 and 56 mole % mesogen-containing units mixed with backbone units without mesogens.[10] In particular, we will address the consequences of the copolymer structure on the dielectric relaxations in these materials.

## EXPERIMENTAL

Three liquid crystalline polymer samples, one poly(methylsiloxane) and two poly(methylsiloxane-*co*-dimethylsiloxane)s containing 2-[4-(2(*S*)-methyl-1-butoxy)-

phenyl]-5-(11-undecanyl)-1,3,2-dioxaborinane side groups, were provided by Professor Percec's group at Case Western Reserve University.[10,25] The samples contain a mesogen attached via an eleven-methylenic spacer to a siloxane beckbone, see Figure 1. The homopolymer has a degree of polymerization (*DP*) of approximately 23 ($x \approx 23$, $y \approx 0$). This *DP* is high enough so that the thermal transitions are independent of molecular weight. The copolymer samples have respectively 35% and 56% mole fraction of mesogenic units. The 35% copolymer has $DP \approx 45$ ($x \approx 16$, $y \approx 29$) and the 56% copolymer has $DP \approx 100$ ($x \approx 56$, $y \approx 44$). Differential scanning calorimetric measurements (DSC) were taken for each of the three samples on a DuPont model 910. Repeated runs show consistency in the position of the mesogenic phase transitions, but the glass transitions vary as expected with thermal history. The transition temperatures of each phase are shown in Table I. The liquid crystalline phase recognitions are based on polarizing optical microscopy studies. All three samples show two smetic phases between the glass transition and the clearing point or isotropic transition. The higher temperature smectic phase is smectic-$C^*$ phase. The lower temperature smectic phase is not yet conclusively identified.

The samples were vaccum cast above the clearing point onto three-terminal brass cells. The 50-μm kapton spacers were placed between the high electrode and the guard ring. The individual brass sample cells were placed in a four-sample holder which was mounted in a cryostat for data collection at low temperatures and a vaccum oven for data collection at elevated temperatures. The temperature in both the cryostat and vacuum oven was controlled by a Lakeshore Model DRC 82C temperature controller

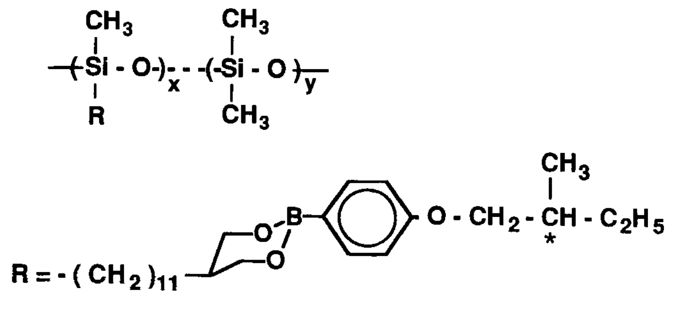

FIGURE 1 Chemical structure of polymethylsiloxane based side-chain liquid crystal homopolymer and copolymer.

TABLE I

Phase Transition Temperature (K) in the Studied Liquid Crystal Polymers

| Sample | $\overline{\text{DP}}$ |  | Glassy | Smectic | Smectic-$C^*$ | Isotropic |
|---|---|---|---|---|---|---|
|  | $x$ | $y$ | $T_{g'}$ | $T_g$ | $T_{s-s_c^*}$ | $T_i$ |
| Homopolymer | 23 | 0 |  | 274 | 294 | 360 |
| 56% Copolymer | 56 | 44 | 207 | 268 | 282 | 345 |
| 35% Copolymer | 16 | 29 | 193 | 261 | 276 | 307 |

with two platinum temperature sensors. Dielectric loss and capacitance data were taken at 17 frequencies (10 Hz to 100 kHz in linear logarithm) on an ultra-precision ratio-arm transformer bridge (CGA-83, Andeen and Assoc.[26]) at 5 K intervals from 200 K to 450 K. Individual sample cells were connected sequentially to the bridge via a Keithley Model 705 RF switch.[27]

## RESULTS

Dielectric loss spectra for the homopolymer, 56% copolymer and 35% copolymer in the smectic phases are shown in Figures 2, 3, and 4, respectively. The homopolymer and the 56% copolymer appear to have both the high-frequency $\alpha$ process and the low-frequency $\delta$ process. The 35% copolymer in Figure 4 exhibits only one process observed.

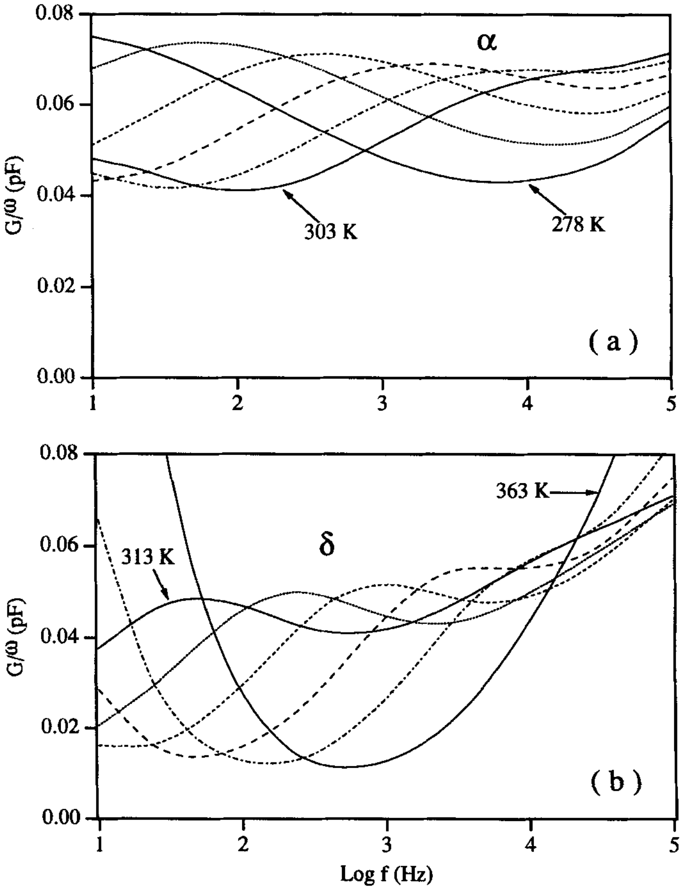

FIGURE 2 Dielectric loss ($G/\omega$) spectrum for the homopolymer. (a) The high-frequency $\alpha$ process from 278 to 303 K in 5 K steps; (b) the low-frequency $\delta$ process from 313 to 363 K in 10 K steps.

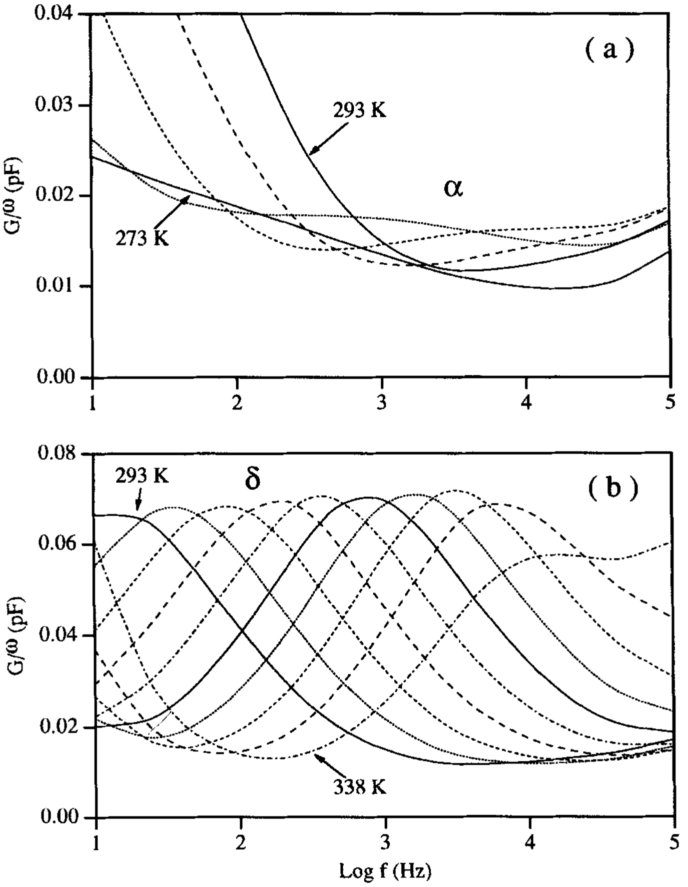

FIGURE 3 Dielectric loss data for the 56% copolymer shown in 5 K steps. (a) The α process (273–293 K); (b) the δ process (293–338 K).

To obtain accurate information on the individual processes the loss data is fit to empirical lineshapes as a function of frequency over the entire range of temperatures. At each temperature the data is modeled with a fitting function using a Levenberg–Marquardt minimization technique.[28] A sum of Fuoss–Kirkwood model functions is used for the fitting function.[24] The Fuoss–Kirkwood function for a single dielectric loss peak is given by

$$\frac{G}{\omega} = L_m \cosh^{-1}[\beta \ln(\omega/\omega_R)] \tag{1}$$

where, $G/\omega$ is the dielectric loss (conductance $G$/angular frequency $\omega = 2\pi f$), $\omega_R = 2\pi f_R$ is the relaxation frequency, $L_m$ is the amplitude, and $\beta$ is the width parameter. The symmetric Fuoss–Kirkwood model is convenient because the amplitude and width are each governed by a single parameter. The area of the peak is simply

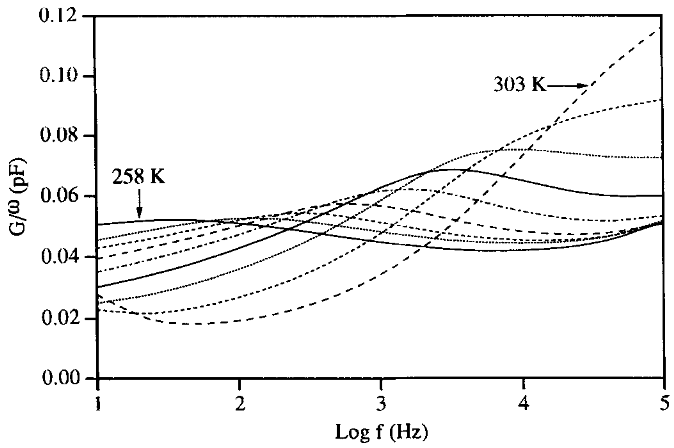

FIGURE 4 Dielectric loss data for the 35% copolymer shown in 5 K steps (258–303 K). Only one mesophase relaxation peak is observed.

$\pi L_m/\beta$, which is proportional to the *dielectric relaxation strength*,

$$\Delta\varepsilon' \equiv \varepsilon'_0 - \varepsilon'_\infty = 2\varepsilon''_m/\beta \tag{2}$$

while $\varepsilon''_m = L_m/C_0$, $\varepsilon'_0$ and $\varepsilon'_\infty$ are the dielectric constants at low-end and high-end frequencies.[14] The dielectric data has been fit over the entire temperature range without difficulty so as to obtain the relaxation frequency $f_R$, width parameter $\beta$ and loss amplitude $L_m$ in Equation (1). The d.c. conductivity was not measured but was assumed to be ohmic and fit where significant.

The resulting relaxation frequencies for the three samples are summarized in Figure 5, which is an Arrhenius plot in terms of reciprocal temperature. All the curves for the $\alpha$ process in Figure 5 show strong downward trends in approaching the glass transition. This sort of molecular dynamic phenomena are called *glassy* or *non-Arrhenius behavior*[29] and are often studied by Williams–Landel–Ferry (WLF) equation or Vogel–Fulcher (VF) equation.[30] The WLF equation is,

$$\mathrm{Log}_{10}\left[\frac{f_R(T)}{f_0(T_0)}\right] = \frac{A(T-T_0)}{B+T-T_0}, \tag{3}$$

where, $A$ and $B$ are constants and for a wide variety of polymers $A = 8.66$ and $B = 101.6$ when $T_0 = T_g + 50\,\mathrm{K}$, $f_R$ is the relaxation frequency at an individual temperature $T$.[31] Meanwhile the VF equation, given by

$$f_R = f^0 \exp[-C/(T-T_\infty)], \tag{4}$$

can also be used to study this glassy behavior. Here $f^0$ is a very high usually between $10^{10}$ Hz and $10^{12}$ Hz, may also be a polynomial function of temperature; $T_\infty$ is

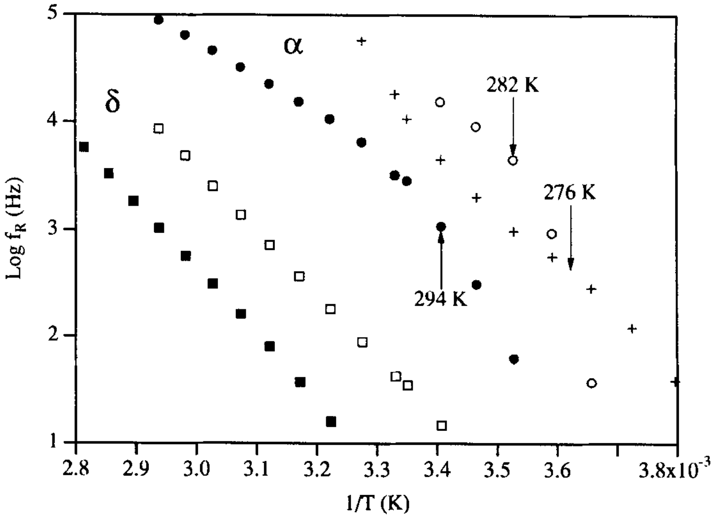

FIGURE 5 Arrhenius plot obtained from Fuoss–Kirkwood data fitting Equation (1). ●, homopolymer α process; ■, homopolymer δ process; ○, 56% copolymer α process; □, 56% copolymer δ process; +, 35% copolymer. Arrow indicates the smectic–smectic-$C^*$ transition temperature $T_{s-s_c^*}$ for each sample.

sometimes called Vogel temperature with $T_\infty < T_g$. The VF equation is a three-parameter fit ($A, B$, and $T_\infty$) whereas the WLF equation is essentially a one-parameter fit (only $T_0$). However the interpretation of the Vogel temperature $T_\infty$ in terms of glass transition is not very clear.[32]

Figure 6 demonstrates the α processes for the homopolymer and 56% copolymer being fit to WLF Equation (3) and VF Equation (4). The WLF equation gives a poor fit. This is not entirely surprising considering the complexity of the side groups of these systems compared to the polymers from which the WLF constants $A$ and $B$ were derived.[31] On the other hand, the VF equation is able to fit the data well and the fitting parameters are, $f^0 \approx 10^{6.5}$ Hz, $C \approx 317$ K and $T_\infty \approx 254$ K for the homopolymer; $f^0 \approx 10^{5.2}$ Hz, $C \approx 65$ K and $T_\infty \approx 266$ K for the 56% copolymer.

## Homopolymer

The two smectic phases seen via DSC in the homopolymer lie between the glass transition at about 274 K and the clearing point at 360 K, see Table I. In this range the dielectric results show the two processes α and δ, see Figure 2. The α process is visible in the frequency range of this experiment from about 275 K to 325 K. The δ process appears together with the high temperature part of the α process above 305 K and is visible up to the clearing point. Above the clearing point the δ peak rapidly diminishes corresponding to a shift to higher frequencies. Clear from the Arrhenius plot for the resolved α and δ processes in Figure 5, the δ peaks cover the entire smectic-$C^*$ phase and the α peaks cover both smectic phases. The δ peak seems linear with an activation energy 118 kJ/mole, which is proportional to the slope in the Arrhenius plot. As

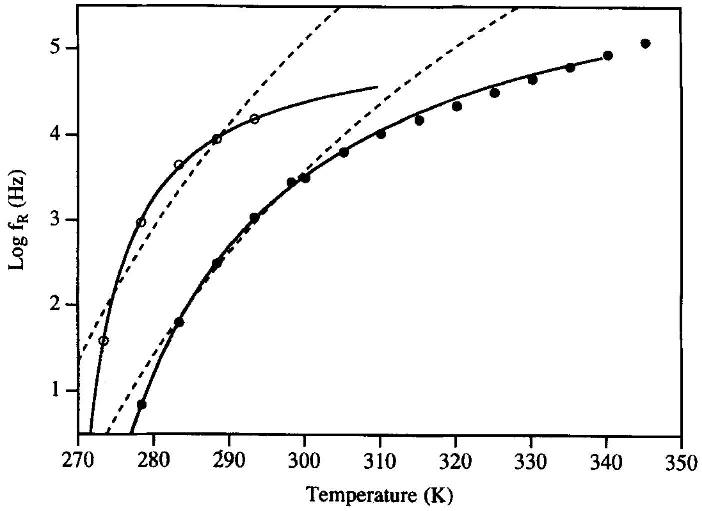

FIGURE 6 The α processes for the homopolymer (●) and the 56% copolymer (○) fit by WLF Equation (3) (----) and by VF Equation (4) (———).

mentioned above, the α process shows strong non-Arrhenius behavior approaching $T_g$. Its activation energy is temperature dependent and increases rapidly toward $T_g$.

A useful point of reference to compare the peak frequencies and the separation between peaks is the smectic–smectic-$C^*$ transition temperature $T_{s-s_c^*}$, see Table I. At this temperature both α and δ peak frequencies can be obtained directly from the data or by extrapolating from the Arrhenius plot in Figure 5. The $T_{s-s_c^*}$ is approximately 294 K for the homopolymer, at which the δ peak is at approximately $10^0$ Hz and the α peak is at $10^{3.1}$ Hz. The separation of the two peaks can be expressed as the ratio of the frequencies at this temperature, and that is about $10^{3.1}$.

## Copolymer

The two smectic phases in the 56% copolymer lie between the glass transition at 268 K and the clearing point at 345 K, see Table I. Both the α and δ processes are seen in this temperature region, see Figure 3. The δ process is seen clearly from 293 K up to the clearing point, at which it is again seen to rapidly diminish. It probably exists in the isotropic phase but at a much higher frequency. Both peaks have again been well fit by the symmetric Fuoss–Kirkwood functions in Equation (1) and the results are shown in Figure 5. At smectic–smectic-$C^*$ transition temperature $T_{s-s_c^*}$ ($\approx 282$ K) the δ peak is at approximately $10^{0.5}$ Hz and the α peak is at $10^{3.5}$ Hz, with a separation of about $10^{3.0}$. Overall, in terms of the temperature/frequency position, the α and δ peaks in the 56% copolymer have about the same separation and temperature dependence as the homopolymer. The only difference is a shift towards higher relaxation frequency by about one decade for the 56% copolymer at a certain temperature, in accord with the lower transition temperature in the copolymer. The Arrhenius plot shows almost no curvature for the $\delta$ process and strong curvature for the $\alpha$ process, see Figure 5. An activation energy for the $\delta$ process is estimated to be 112 kJ/mole, about 5% lower than that for the homopolymer. The $\alpha$ process was also fit to a WLF equation with poor results (Figure 6). Again the VF equation fits well and is probably due to the three adjustable parameters.

The most striking difference between the 56% copolymer and the homopolymer is the size of the $\alpha$ process. As shown in Figure 3, the $\alpha$ process for the 56% copolymer is much smaller relative to the $\delta$ process, and is only barely visible between $T_\infty$ and $T_{s-s_c^*}$. Because of this, it is difficult to resolve the $\alpha$ process at higher temperatures (above 10 kHz) where it should still be visible. At lower temperatures the $\alpha$ peak may be seen approaching the glass transition, near which it broadens considerably.

As mentioned above, like the homopolymer and 56% copolymer, the 35% copolymer shows two smectic phases between the glass transition $T_g$ ($\approx 261$ K) and the isotropic transition $T_i$ ($\approx 307$ K), see Table I. However there is only one relaxation process observed in this temperature region (Figure 4), and the single peak is well fit by a single Fuoss–Kirkwood function, see Equation (1). The smectic–smectic-$C^*$ transition $T_{s-s_c^*}$ occurs at 276 K. The relaxation appears between the second glass transition $T_{g'}$ and up to the isotropic transition $T_i$. The Arrhenius plot of this single peak seems not decreasing monotonically, see Figure 5. As such it is fit by neither a straight line (Arrhenius equation) nor any glassy description, i.e., WLF or VF equations. The activation energy is estimated to be 120 kJ/mole on the average.

## DISCUSSION

There are two main points of interest in the above description of the dielectric spectra of these materials, the rapid decrease in the area of the $\alpha$ process relative to the $\delta$ process in the 56% copolymer compared with the homopolymer and the presence of only a single process in the 35% copolymer. The two phenomena appear to be related.

The dielectric relaxation strength $\Delta\varepsilon'$, proportional to the area under the dielectric loss peak, correlates with the average dipole moment per unit volume relaxed by the process.[30] The relative size of the $\alpha$ process compared with the $\delta$ process is much smaller in the 56% copolymer (Figure 3) than in the homopolymer (Figure 2). In liquid crystals the dipole moment per unit volume relaxed by a dielectric process is a function of both the magnitude and orientation of the director.[33] If only the magnitude of the director, which represents the degree of order in the liquid crystal region, were significantly different in the 56% copolymer compared to the homopolymer, then one would expect both the $\alpha$ process and $\delta$ process to be affected approximately equally by copolymerization. As this is not the case we are led to believe that the orientation of the director is the primary difference in the copolymer. The samples were prepared without any special surface treatment and are expected to be multi-domain samples, with the individual liquid crystal domains randomly oriented. We believe that in the 56% copolymer the domains are preferentially ordered by the untreated brass surfaces in a homeotropic alignment.[34] Given the same surface condition, the 56% copolymer may be more affected due to its lower vescosity. This would explain the diminished $\alpha$ process as the $\alpha$ process is missing in a perfectly aligned homeotropic SCLCP.[20,21,34]

As the samples are in opaque brass sample cells, it is not possible to observe directly the degree of alignment. One test of alignment effects which was attempted was to change the rate at which the samples were cooled from the isotropic phase. The samples were heated to temperatures above the isotropic transition and rapidly quenched to 80 K. No effect on the relative size of the $\alpha$ and $\delta$ peaks was observed.

The other point of interest is the observation of the single process in the 35% copolymer. However, the $\alpha$ and $\delta$ processes in the 35% copolymer may both be present but unobservable because of their closeness in frequency, that is, strong overlap. The Arrhenius plot of a composite peak consisting of two peaks with different apparent activation energies and comparable peak amplitudes at each temperature would display unusual curvature, see Figure 5. The notion of overlapped peaks in copolymers is consistent with the homopolymer/copolymer pair studied by Haws *et al.*[22]

The single observed peak in the 35% copolymer occurs at $10^{2.6}$ Hz at smectic–smectic-$C^*$ transition $T_{s-s_c^*}$ ($\approx 276$ K). As one generally expects the $\delta$ process to always be at a somewhat lower frequency than the $\alpha$ process, the $\delta$ process would be expected at a frequency somewhat lower than $10^{2.6}$ Hz but no more than about 0.5 decade, and the $\alpha$ process would be expected at a frequency somewhat higher than $10^{2.6}$ Hz. At a similar $T_{s-s_c^*}$, the $\alpha$ process is at $10^{3.1}$ Hz in the homopolymer and $10^{3.5}$ Hz in the 56% copolymer. The frequency of the $\alpha$ process in the 35% copolymer would seem a little bit low, probably between $10^{2.6}$ and $10^{3.1}$ Hz. The frequency of the $\delta$ process, extrapolated from Arrhenius Figure 5, is $10^{0}$ Hz in the homopolymer and $10^{0.5}$ Hz in the 56% copolymer. In the 35% copolymer there is then a significant increase in the frequency of the $\delta$ process to a value probably between $10^{2.1}$ and $10^{2.6}$ Hz. In other words, the separation between *two peaks* in the 35% copolymer at $T_{s-s_c^*}$ is less than one decade compared with approximately 3.1 decades for the homopolymer and 3.0 decades for the 56% copolymer.

As mentioned in the introduction, the $\delta$ process is thought to be rotations of the longitudinal dipole moment of the side-chain mesogen about its short axis, and in the smectic phase it is possible for the mesogen to rotate around the polymer backbone, hopping from one layer to another.[17] It is likely that such a large motion requires cooperation of the backbone segments with the mesogen. A large increase in the frequency of the $\delta$ process for the two copolymers indicates easier cooperative motion for the polymer backbone. That is, in the copolymer, the backbone can rearrange itself more easily to accommodate the reorienting mesogen, resulting in a faster process. This change is not very apparent in the 56% copolymer, where there is a mesogen containing side group on approximately 1/2 of the backbone segments, but becomes quite pronounced in the 35% copolymer, in which 1/3 of the backbone segments have mesogenic side groups. We also note that in the homopolymer one would expect the layers containing backbones to be more densely filled. This might be expected to impede and slow down the $\delta$ process. From this viewpoint, the increased cooperativity of the backbone with the mesogen in copolymers is quite obvious.

Finally it is remarkable how similar the dielectric spectrum of the homopolymer from this study is with the dielectric spectrum of the SCLCP studied extensively by Attard and Willium *et al.*,[20] especially considering their very different mesogens and different spacer lengths (8 versus 11). Their smectic sample has transition temperatures nearly identical to the homopolymer in this study—the glass transition 274 K and the clearing point 363 K. The apparently higher activation energies for both α and δ processes in their sample is primarily due to a shorter methylenic group attached to the side of the phenyl ring, resulting in more coupling between the mesogen and the backbone.[35] This shorter spacer may also serve to increase the hindering of long axis rotations by the polymer backbone.

## CONCLUSION

The copolymer morphology in a side-chain liquid crystal system decreases the amplitude of the high-frequency α process relative to the low-frequency δ process, probably through surface induced homeotropic alignment. Additionally in the copolymers both the α and δ processes are shifted to higher frequencies at a given temperature. In the 35% copolymer the δ process is shifted more than the α processes resulting in the two processes becoming overlapped. These observations suggest that the copolymer structure has a greater effect on large scale reorientations of the mesogen because of the increased cooperation with the backbone.

### Acknowledgement

This work was supported by the NSF Materials Research Group at CWRU under grant DMR 89-01845. Support for Z. Z. Z. came from NSF Science and Technology Centre for Advanced Liquid Crystalline Optical Materials (ALCOM) under grant DMR 89-20147. The authors thank Virgil Percec and Bruce Hahn for providing samples and Rolfe Petschek for helpful descussions.

### References

1. H. Finkelmann, M. Portugall and H. Ringsdorf, *Am. Chem. Soc., Div. Polym. Chem.*, **19**, 183 (1978); H. Finkelmann, D. Naegele and H. Ringsdorf, *Makromol. Chem.*, **180**, 803 (1979).
2. N. A. Platé and V. P. Shibaev, *Comb-Shaped Polymers and Liquid Crystals* (Plenum Press, New York, 1987), Chap. 4, pp. 199–415.
3. M. Engel, B. Higen, R. Keller, W. Kreuder, B. Reck, H. Ringsdorf, H.-W. Schmidt and P. Tschirner, *Pure and Appl. Chem.*, **57**, 1009 (1985).
4. V. Percec and C. Pugh, in *Side Chain Liquid Crystal Polymers* (Chapman, New York, 1989), C. B. McArdle, Ed., Chap. 3, pp. 30–105.
5. V. P. Shibaev, in *Liquid-Crystal Polymers* (Plenum Press, New York, 1993), N. A. Platé, Ed., Chap. 6, pp. 193–249.
6. V. P. Shibaev, *Mol. Cryst. Liq. Cryst.*, in press.
7. B. Hahn and V. Percec, *Macromolecules*, **20**, 2961 (1987).
8. V. Percec, *Mol. Cryst. Liq. Cryst.*, **155**, 1 (1988).
9. B. Hahn and V. Percec, *Mol. Cryst. Liq. Cryst.*, **157**, 125 (1988).
10. V. Percec and B. Hahn, *Macromolecules*, **22**, 1588 (1989).
11. Z. Z. Zhong, D. E. Schuele, W. L. Gordon, K. J. Adamic and R. B. Akins, *J. Polym. Sci.*, **B30**, 1443 (1992)
12. H. Kresse, E. Tennstedt and R. Zentel, *Makromol. Chem., Rapid Commun.*, **6**, 261 (1985).
13. L. Monnerie, F. Lauprêtre and C. Noël, *Liq. Crystals*, **3**, 1013 (1988).
14. C. M. Haws, M. G. Clark and G. S. Attard, in *Side Chain Liquid Crystal Polymers* (Chapman, New York, 1989), C. B. McArdle, Ed., Chap. 7, pp. 196–223.
15. P. L. Nordio, G. Rigatti and U. Segre, *Mole. Phys.*, **25**, 129 (1973).
16. G. S. Attard, *Molec. Phys.*, **58**, 1087 (1986).
17. K. Araki, G. S. Attard, A. Kozak, G. Williams, G. W. Gray, D. Lacey and G. Nestor, *J. Chem. Soc. Faraday Trans. II*, **84**, 1067 (1988).
18. A. Kozak, J. K. Moscicki, G. Williams, *Mol. Cryst. Liq. Cryst.*, **201**, 1 (1991).
19. R. Zentel, G. R. Strobl and H. Ringsdorf, *Macromolecules*, **18**, 960 (1985).

20. G. S. Attard, J. J. Moura-Ramos and G. Williams, *J. Poym. Sci.*, **B25**, 1099 (1987).
21. H. Pranoto, F.-J. Bormuth and W. Haase, *Makromol. Chem.*, **187**, 2453 (1986); F.-J. Bormuth and W. Haase, *Mol. Cryst. Liq. Cryst.*, **148**, 1 (1987); F.-J. Bormuth and W. Haase, *Liq. Cryst.*, **3**, 881 (1988).
22. C. M. Haws, M. G. Clark and C. B. McArdle, *Mol. Cryst. Liq. Cryst.*, **153**, 537 (1987).
23. The homopolymer "A" was studied by Attard and Williams, *et al.*, see reference [20] above, and that data is presented alongside the equivalent copolymer in the paper [22] by Haws, *et al.*
24. R. M. Fuoss and J. G. Kirkwood, *J. Am. Chem. Soc.*, **63**, 385 (1941).
25. B. Hahn, *Synthesis of Polymers with Potential Ferroelectric Properties*, (Ph.D. Thesis, Case Western Reserve Unviersity, Cleveland, 1988).
26. C. G. Andeen, *Accurate Determination of Dielectric Properties*, (Ph.D. Thesis, Case Western Reserve University, Cleveland, 1971).
27. Z. Z. Zhong, *Dielectric Relaxations in Side-Chain Liquid Crystalline Polymers* (Ph.D. Thesis, Case Western Reserve University, Cleveland, 1993).
28. W. H. Press, B. P. Flannery, S. A. Teukolsky and W. T. Vetterling, *Numerical Recipes* (Cambridge University Press, London, 1986).
29. Z. Z. Zhong, D. E. Schuele, S. W. Smith and W. L. Gordon, *Macromolecules*, **26**, 6403 (1993).
30. N. G.McCrum, B. E. Read and G. Williams, *Anelastic and Dielectric Effects in Polymeric Solids* (Dover Publications, New York, 1991).
31. M. L. Williams, R. F. Landel and J. D. Ferry, *J. Am. Chem. Soc.*, **77**, 3701 (1955).
32. W. M. Saslow, *Phys. Rev.*, **B37**, 676 (1987).
33. S. Chandrasekhar, *Liquid Crystals* (Cambridge University Press, Cambridge, 1992).
34. Z. Z. Zhong, W. L. Gordon, D. E. Schuele, R. B. Akins and V. Percec, *Mol. Cryst. Liq. Cryst.*, **238**, 129 (1994).
35. Z. Z. Zhong, D. E. Schuele and W. L. Gordon, *Liq. Crystals*, in press.